Isı Emicilerin Geometrik Parametrelerinin ve Akışkan Özelliklerinin Soğutma Üzerindeki Etkisinin RSM Yöntemi İle İncelenmesi

Taha Tuna GÖKSU[1*] iD

[1]Makine Mühendisliği, Mühendislik Fakültesi, Adıyaman Üniversitesi, Adıyaman, Türkiye.
[1]tgoksu@adiyaman.edu.tr

Öz

Bu çalışma, blok tiplerinde ve çeşitli akışkanlar kullanılarak tasarlanan ısı alıcıları üzerinde yanıt yüzey yöntemi (RSM) etkisini araştırmaktadır. RSM yöntemi, su, mono-nanoakışkanlar ve hibrit nanoakışkanlar kullanılarak hem dikey hem de yatay yönlerde yerleştirilen blok tipinde tasarlanan ısı emicilerinden elde edilen verilere uygulanmıştır. Veriler beş farklı basınç sınır koşulu altında toplanmış ve 144 veri setine uygulanmıştır. Tasarım parametrelerini analiz etmek ve yedi farklı parametre için denklemler türetmek için Box-Behnken yöntemi kullanılmıştır: yoğunluk, viskozite, özgül ısı, termal iletkenlik, blok kalınlığı, blok mesafeleri ve giriş basıncı sınır koşulları kullanılan parametrelerdir. Denklemler ortalama CPU sıcaklığını, termal direnci ve Performans Değerlendirme Kriterlerini (PEC) belirlemek için kullanılmıştır. Sonuçlar, yatay düzenlemelerde termal direnç (R_{th}), CPU ortalama sıcaklık (T_m) ve Performans Değerlendirme Kriteri (PEC) için R^2 değerlerinin sırasıyla %99.21, %99.21 ve %99.37 olduğunu göstermektedir. Dikey olarak tasarlanan geometrilerdeki R^2 değerleri %97.66, %97.66 ve %98.45 olup FLUENT'ten elde edilen sonuçlar ile ANOVA istatistiksel sonuçları arasında güçlü bir korelasyon olduğunu göstermektedir. Her bir değişkenin doğrusal, kare ve kübik etkileri her bir çözümü önemli ölçüde etkilemiştir. Çalışma, RSM yönteminin, yatay düzenlemelerde daha yüksek R^2 değerleri ve bloklar arasında daha yüksek mesafe ile ısı alıcıları üzerinde önemli bir etkiye sahip olduğu sonucuna varılmıştır. Bir diğer önemli sonuç ise blok kalınlığının artmasının da R_{th} ve T_m üzerinde önemli bir etkiye sahip olduğunu göstermiş, soğutma kapasitesini de artırırken sıcaklık dağılımını homojenleştirdiği görülmüştür.

Anahtar kelimeler: Isı emicisi, RSM, Mono-hibrit nano akışkan, PEC

---

*Yazışılan yazar

Investigation of The Effect of Geometrical Parameters And Fluid Properties of Heat Sinks on Cooling By RSM Method

Taha Tuna GÖKSU[1*] (iD)

[1]Mechanical Engineering Department, Engineering Faculty, Adiyaman University, Adiyaman, Türkiye.
[1]tgoksu@adiyaman.edu.tr

Abstract

This study investigated the effect of the response surface method (RSM) on heat sinks designed in block types and using various fluids. The RSM method was applied to the data obtained from heat sinks designed in block type placed in both vertical and horizontal directions using water, mono, nanofluids, and hybrid nanofluids. The data were collected under five different pressure boundary conditions and applied to 144 data sets. The Box-Behnken method was used to analyze the design parameters and derive equations for seven different parameters: density, viscosity, specific heat, thermal conductivity, block thickness, block distances, and inlet pressure boundary conditions. The equations were used to determine the average CPU temperature, thermal resistance, and Performance Evaluation Criteria (PEC). The findings show that the R^2 values for thermal resistance (R_{th}), average CPU temperature (T_m), and performance evaluation criteria (PEC) for flat arrangements are 99.21%, 99.21%, and 99.37%, respectively. The R2 values for the vertically designed geometries are 97.66%, 97.66%, and 98.45%, indicating a strong correlation between the results obtained from FLUENT and the ANOVA statistical results. The linear, square, and cubic effects of each variable had a significant impact on each solution. The study concluded that the RSM method has a significant effect on heat sinks with higher R^2 values in horizontal arrangements and a higher distance between blocks. Another important result showed that increasing the block thickness also has a significant effect on R_{th} and T_m, homogenizing the temperature distribution while increasing the cooling capacity.

Keywords: Heat sink, RSM, Mono-hybrid nanofluid, PEC

---

1. Introduction

Electrical equipment that experiences thermal issues must be cooled passively using cost-effective and efficient thermal conductors, such as pin or plate fin heat sinks [1–6]. Researchers Chiu et al. [7,8] investigated the cooling efficiency of circular pin-type heat. Size, shape, amount, arrangement, location, and kind of coolant are some of the many factors that significantly impact a heat sink's effectiveness. Researchers have studied the cooling capacity of heat sinks with many fins using numerical analysis. Results from CFD (Computational Fluid Dynamics) models demonstrate that double-stack configurations dissipate heat more effectively than single-stack designs. The rib cavity, which is the investigation of the effect of the gap between the pin-type designed geometries, has shown to be an incredibly effective tool for creating innovative designs. It is critical to modify the width of the aluminum band and the placement of the connections, and perforated structures improve heat transfer in heat sinks. A lower thermal resistance and a higher Nusselt number are seen in mini-channel heat sinks (Nu). According to their findings, cooling efficiency is improved when phase-change materials and synthetic jets are used [9–23]. Nanofluids are being used more and more to improve heat transfer in different heat sink setups because of their excellent thermal conductivity and density. Kavitha et al.'s computational research [24] showed that using an Al_2O_3/water nanofluid significantly enhanced heat transfer for a fin-type heat sink by 68%. The idea of utilizing nanoparticles in coolant was first put forth by Choi [25]. To enhance heat control in electronic applications, Choi and Eastman [26] used nanofluids. The experiment looked at how the Al_2O_3-H_2O nanofluids moved and how they transferred heat in silicon-based trapezoidal microchannels. The experiment looked at how the Al_2O_3-H_2O nanofluids moved and how they transferred heat in silicon-based trapezoidal microchannels. When compared to pure water, the results showed that there was a small increase in pressure drop and flow friction. The Nusselt number exhibited a positive correlation with the concentration of particles, the Reynolds number, and the Prandtl number. The study also investigated nanoparticle clustering and settling in small channels, revealing uncertain heat transport during boiling. The spider web-inspired baseplate design enhanced the CPU's temperature regulation and thermal efficiency [27,28]. The fins were filled with a graphene/water nanofluid. The cooling performance of a mini-channel heat sink with a wavy pattern was examined using supercritical CO_2. Using an input temperature as low as 305 K, the study found that the heat transfer coefficient increased by an astounding 8.58 times [29]. A combination of wavy and square fins on an inclined cooler box with magnetized-radiative nanofluid shows a considerable increase in performance[30,31]. Maximum Nusselt number increases of 23.1 percent, 16.5 percent, and 8 percent were achieved using square, triangular, and circular finned fins that were cooled with nanofluid, respectively [32]. When nanofluids are added to the Eulerian-Lagrangian method, the heat transfer coefficient of a micro pin-fin heat sink is enhanced by sixteen percent [33,34].

Nanofluids comprising Al_2O_3/water and MgO/water were determined to be more efficient than TiO_2/water and Al_2O_3/water in a rectangular microchannel heat sink, according to a research [35]. Ozbalcı et al. [36] found that a cost-effective and energy-efficient method of cooling electronic devices is to combine nanofluids with metal foam. On the topic of solar panel cooling, Karaaslan and Menlik looked into the effects mono and hybrid nanofluids [37]. With volume concentrations of 0.5% and 1%, In their study, Ho et al. [38] investigated the effect of various types of nanofluids on a micro-channel heat sink. They found a significant increase in the heat transfer coefficient of 14.43%. In a research conducted by Sriharan et al. [39], the convective heat transfer coefficient was shown to rise by 40%, 28%, and 22% when using nanofluids Al_2O_3, MgO, and CuO in a hexagonal tube heat sink, respectively. The use of nanofluids to the cooling of heat sinks has been the subject of several investigations. The results demonstrate that, in comparison to more traditional cooling fluids, they possess superior thermal characteristics. Their unique features also contribute to their enhanced heat transfer efficiency, reduced pressure drop, and higher thermal conductivity. Their capacity for practical implementation in various other industries is unquestionable, although encountering certain challenges [40–46,46–48].

Leading researchers, though not frequently, use RSM in the geometrical design of heat sinks. Zhou et al. [49] utilized the RSM method to analyze heat sinks with wavy structures, revealing a 2.8-fold increase in heat transfer compared to straight ducts. Some researchers [50] have used the RSM approach in combination with nanofluid and show several parallels with the presented work, despite the difference in geometrical design. The use of RSM and an artificial neural network to design a micro-channel heat sink

demonstrated that the pareto-optimal design point has better hydraulic and thermal performance than the predefined design [51]. The study [52] focuses on optimizing the design of a heatsink manifold microchannel utilizing MWCNT/water-nanofluid to achieve minimal pressure drop and thermal resistance. The ideal design locations are established through the analysis of the flow field and heat transfer, exhibiting a strong correlation between model predictions and simulation results.

The objective of this study is to examine the impact of RSM on heat sinks that are designed in block types and use various fluids. Several impactful research have employed the RSM method to successfully achieve geometric optimization. The RSM approach is employed to identify the optimal scenario that considers both the geometric impact and the influence of the cooling fluid on the heat sink. The RSM method was applied to data obtained from both vertical and horizontal orientations with different thicknesses (ranging from 0.3–0.6 mm) and gap distances (1–1.5 mm). The fluids used were water, mono-nanofluids (2% volume concentration of CuO/water), and hybrid nanofluids (1% CuO + 1% Fe/water). The data were collected under four different pressure boundary conditions (689, 1370, 2040, and 2750 Pa), resulting in a total of 144 data points. The paper presents a unique value due to the large number of parameters analyzed and the use of the RSM method.

2. Geometry and Boundary Condition

This research investigates eight different heat sink designs in detail using the FLUENT software, all operating under the same boundary conditions. The investigated heat sink designs include a range of thickness (a) values between 0.3 and 0.6 mm, block spacing (s) values between 1 and 1.5 mm, and their matching configurations aligned vertically with the fluid flow. In their experiments, Chiu et al. [7] used a boundary condition of 300 kW/m^2 of heat flux going to the base (10x10 mm^2) of the heat sink, with a temperature of 300 K at the start. Figures 1 and 2 depict the dimensions of the heat sink, which are 4 mm in height, 2.5 mm in block height, and 1.5 mm above the foundation [7]. Table 1 describes the geometric arrangements used in Figure 1. These arrangements are named based on the thickness of the blocks and the distance between them in the vertical and horizontal orientations.
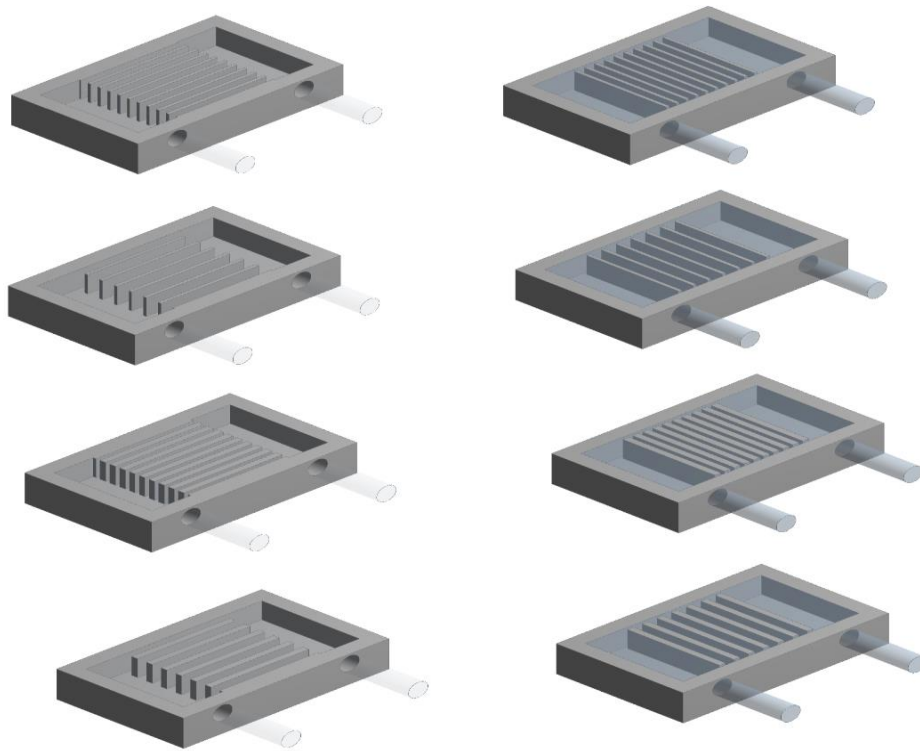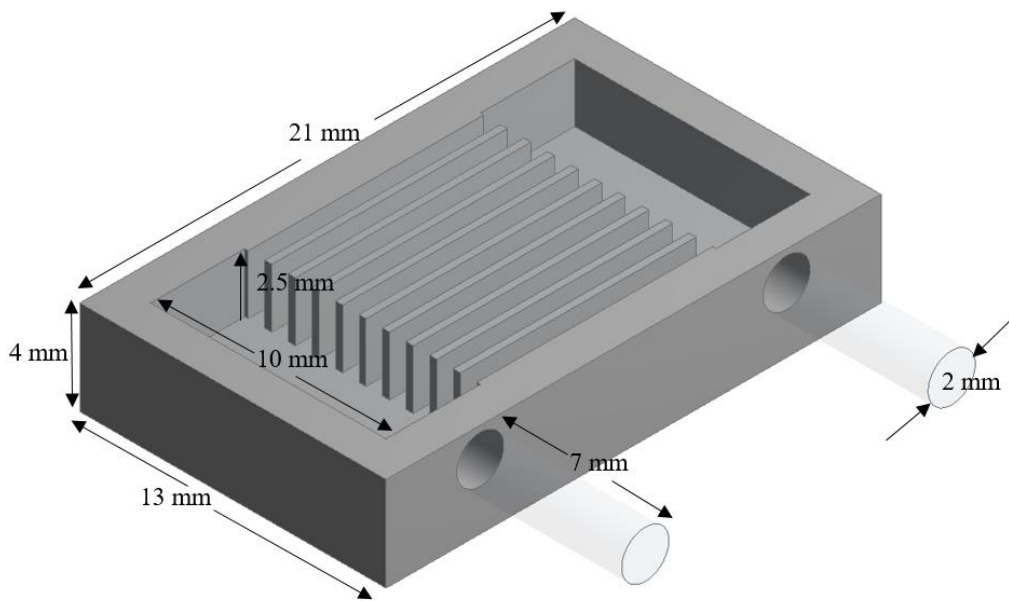

Figure 1. Schematic of heat sinks

Table 1. Named studied heat sinks

Name	Thickness (mm)	Distance (mm)	Orientation
a	0.3	1	Horizontal
b	0.3	1.5	
c	0.6	1	
d	0.6	1.5	
e	0.3	1	Vertical
f	0.3	1.5	
g	0.6	1	
h	0.6	1.5	

Figure 2. Parametric details of geometry

3. Numerical Analysis

This section will describe the method used to obtain the data presented in the previous paper [53] The cooling performance of the heat sink was investigated using the FLUENT program. The k-ε turbulence model and SIMPLE solution method were employed.

The boundary conditions used in this investigation were inlet temperature, pressure, and constant heat flow. A steady heat flux of 300 kW/m², input temperatures of 300 K, pressures of 689, 1370, 2040, 2750, 3450, and 4150 Pa were the precise boundary conditions that were established. A prior study [53] set boundary conditions at 689, 1370, 2040, and 2750 Pa, and collected data accordingly. However, for the Box-Behnken Design in RSM, a minimum of 62 data points is required for 7 distinct input variables. To meet this requirement, fresh data points were collected at pressures of 3450 and 4150 Pa. A total of 72 data sets were analyzed using RSM. Furthermore, every wall of the heat sink was subjected to an adiabatic boundary condition.

Effective thermal resistance is the most important metric for evaluating heat sink performance and cooling efficacy (R_{th}). A lower score indicates that the system is more efficient. Equations 1 and 2 demonstrate the computation of R_{th} and the heat transfer coefficient [54]. Equation 3 defines the Reynolds number, and

Equation 4 computes the friction factor. Equation 5 shows the metric for evaluating performance (PEC). Equation 5 uses the pin structure with a circular cross-section to get the value of parameter a [55].

$$R_{th} = \frac{T_{CPU,m} - T_{in}}{q''} \tag{1}$$

$$h = \frac{q''}{T_{CPU,m} - T_{bf}}_{th} \tag{2}$$

$$Re = \frac{\rho.V.D_h}{\mu}, \tag{3}$$

$$f = \frac{2.\Delta P.D_h}{\rho.L.V^2}, \tag{4}$$

$$PEC = \frac{h_a/h_0}{\left(f_a/f_0\right)^{1/3}}. \tag{5}$$

In this context, the letters 'a' and '0' denote the given geometrical shapes names and experimental research geometry [7] relative to circular geometry, respectively. A better grasp of the working fluid's properties as they relate to flow and heat transmission is the primary goal of this research, which aims to maximize efficiency in thermal systems. The process incorporates nanoparticles of iron (Fe) and copper oxide (CuO) into water, which serves as the base fluid. Because the behavior of hybrid nanofluids is best approximated at lower nanoparticle concentrations, a 2% concentration was determined to be optimal for this study [56]. The previous study [53] provided calculations for the thermophysical properties of mono and hybrid nanofluids.

4. Response Surface Method

Predictive model contrary to conventional optimization methods that overlook communication characteristics and responses, the RSM technique can effectively respond to this interaction, resulting in a reduced number of experiments required for the current work and facilitating more efficient numerical and practical processes. Mostly used in practical applications, the RSM has recently shown its usefulness in computational investigations. It is considered a distinctive method due to its notable benefits, such as expediting the computational process and forecasting nonlinear optimal formulas. This approach demonstrates the correlation between the design aspect and the replies. Response Surface Methodology (RSM) employed the Box-Behnken method. Seven design parameters (density, viscosity, specific heat, thermal conductivity, block thickness, void distances, and inlet pressure boundary conditions) were used to determine the relationship between the three responses R_{th}, T_m, and PEC.

5. Result and Discussions

The Response Surface Method (RSM) was used in this study to analyze the data obtained from using different fluids (nano-fluid and hybrid nano-fluid) in CPU cooling. The block type and eight different geometrical structures (a = 0.3–0.6 mm, s = 1–1.5 mm, vertical and horizontal orientation) were designed and validated with an experimental study [7], as shown in Figure 3. Based on the results obtained, the maximum deviation for R_{th} is below 4.7%, indicating a highly efficient analysis. The

volumetric flow rate showed a maximum deviation of 6.42% between the experimental [7] and numerical studies. In the previous study, four distinct pressures of 689, 1370, 2040, and 2750 Pa were examined. In this study, a minimum of 62 data sets are required for Box-Behnken analysis, considering 7 different parameters. Consequently, new findings were obtained for pressures of 3450 and 4150 Pa in each case. Figures 4, 5, and 6 display all the respective results obtained. The section will be divided into two parts. The first part includes the RSM analysis of the data for different fluids designed in horizontal arrangements, while the second part examines the data for vertical arrangements. The figures clearly show that both R_{th}, T_m, and PEC values increase with increasing inlet pressure boundary conditions. Of course, this is a positive situation for R_{th} and T_m, while the same cannot be said for PEC. For this reason, RSM was performed, and its effect is seen in the equations below. It was seen that the minimum R_{th} was obtained as 0.2563 when mono nanofluid was used, and a=0.6 s=1 mm. Chiu et al. [7,8] found the minimum thermal resistance in pin-type geometries to be 0.258 at P = 5000 Pa in their study, but the presented study found this value to be R_{th} = 0.256 at 4150 Pa, making it a significant contribution to the literature. The reason for its importance is that the mentioned studies are both experimental studies and studies used in verification. It is also seen from Figure 5 that the same geometry provides a more uniform temperature distribution. The maximum PEC of 1.04 was obtained when hybrid nanofluid was used, followed by mono nanofluid with 1.03.
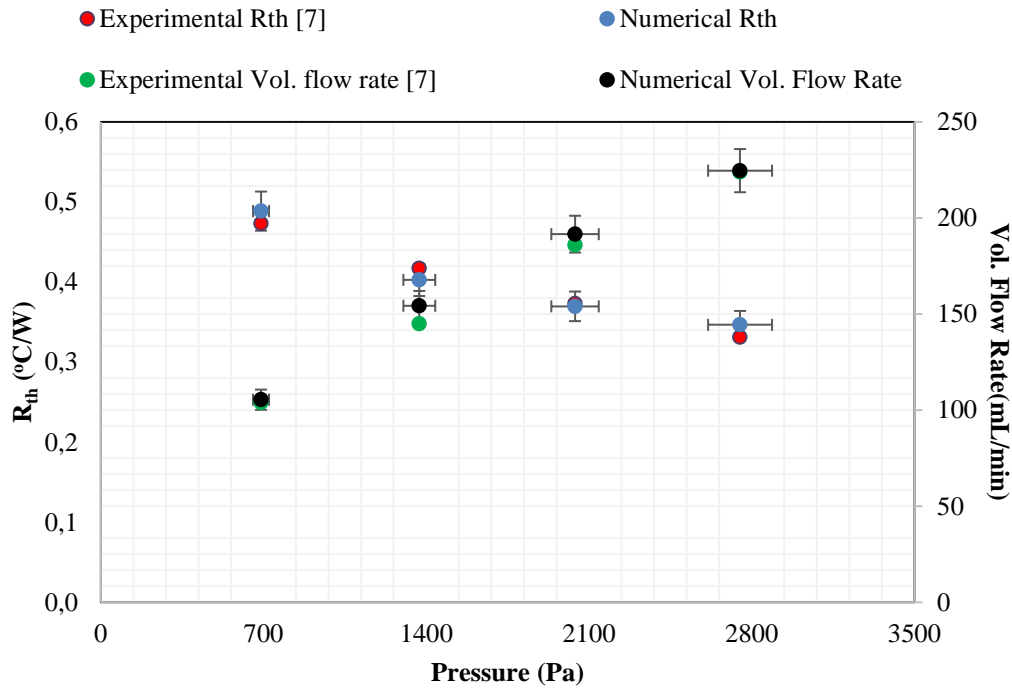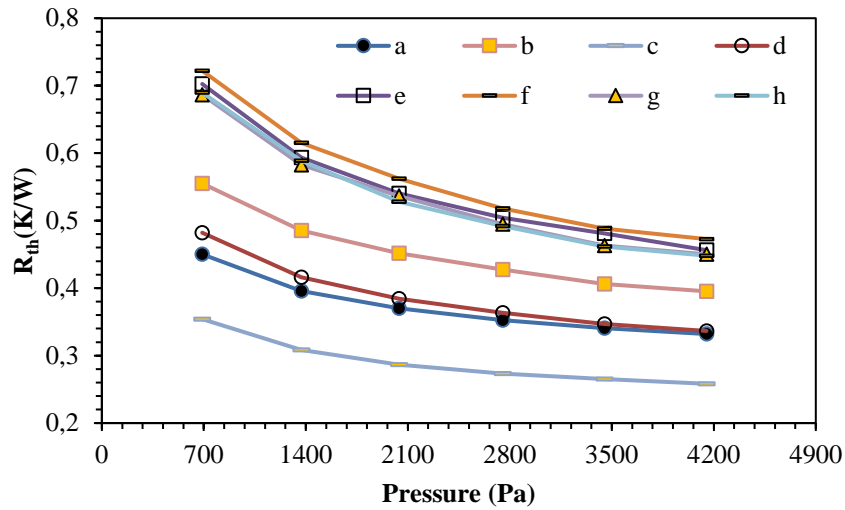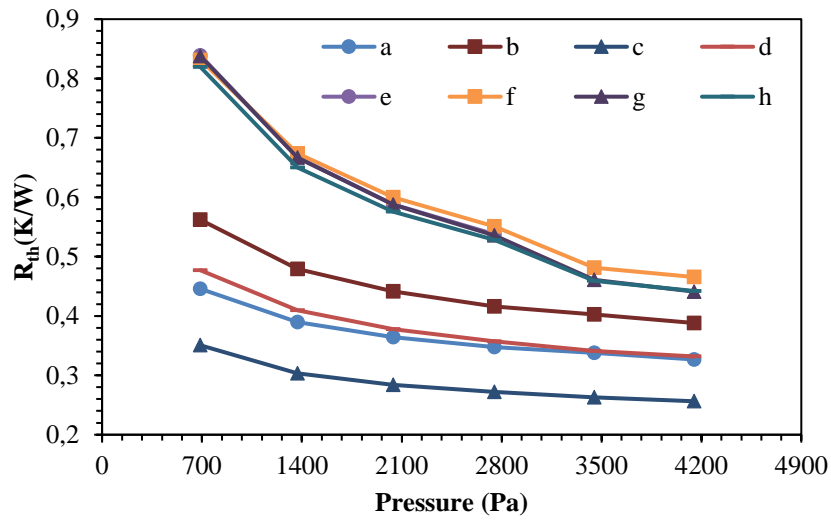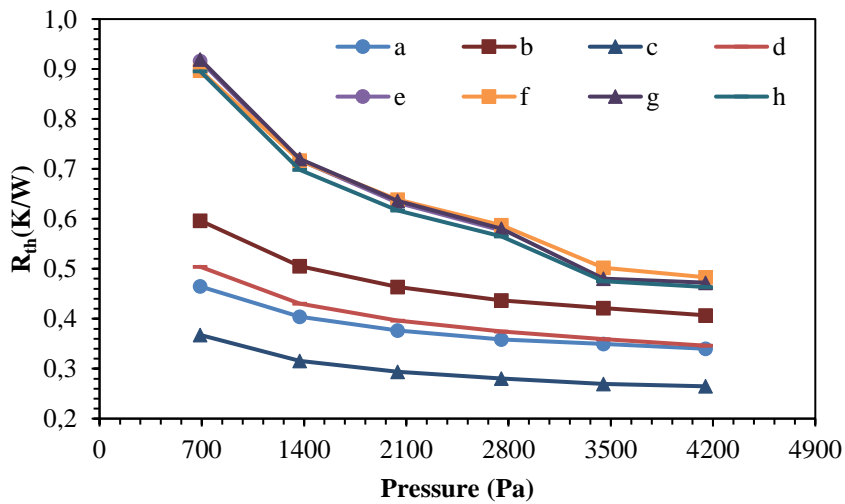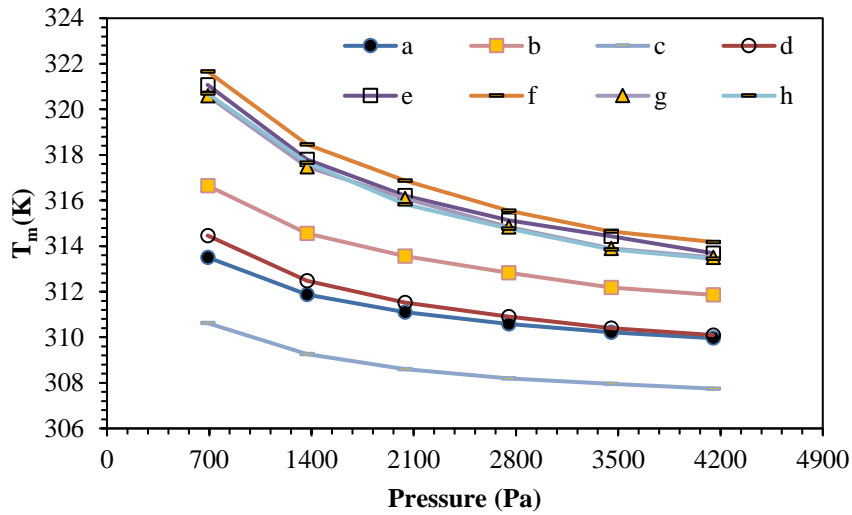

Figure 3. Validation results

(a)

(b)
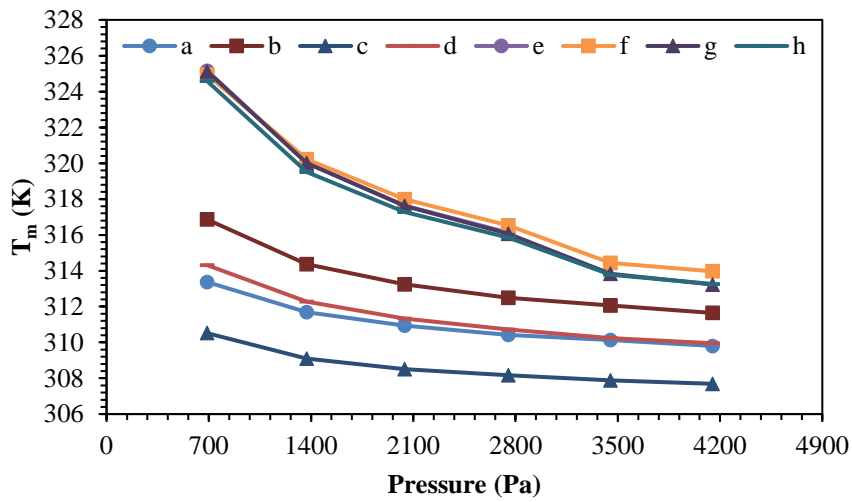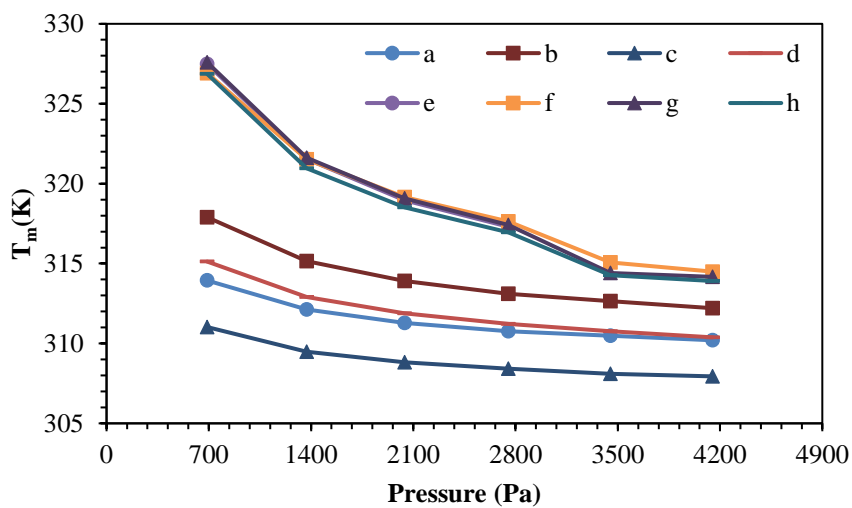

(c)

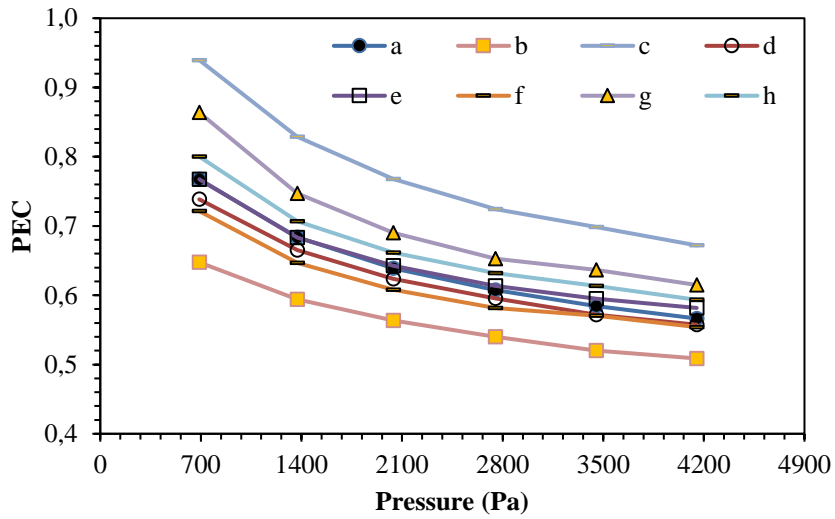**Figure 4.** R_{th} Results of (a) water (b) mono (c) hybrid nanofluids
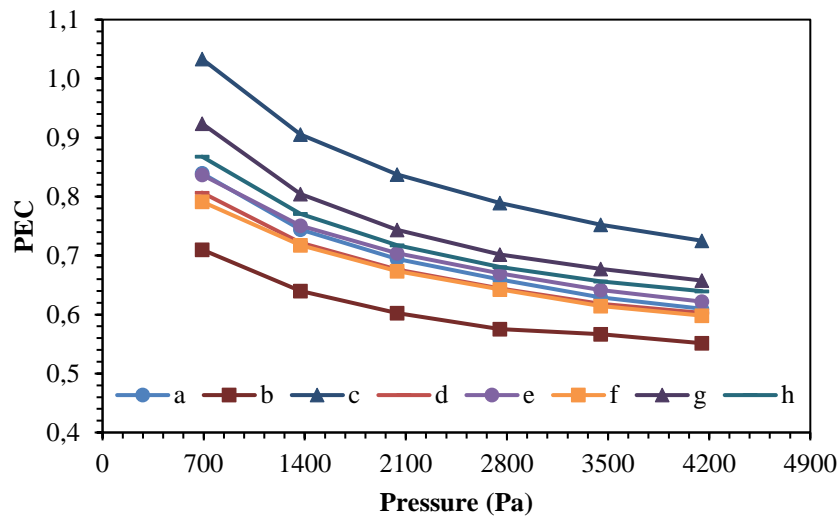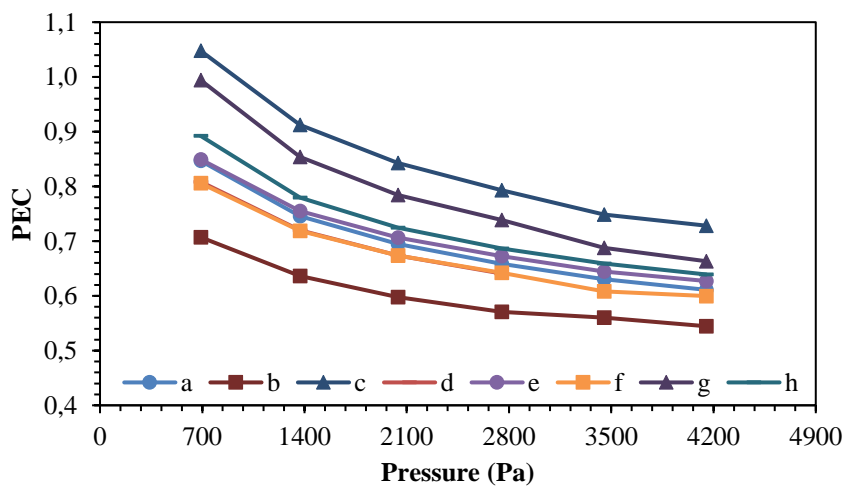
(a)

(b)

(c)

Figure 5. T_m Results of (a) water (b) mono (c) hybrid nanofluids

(a)

(b)

(c)

Figure 6. PEC Results of (a) water (b) mono (c) hybrid nanofluids

5.1. Findings from horizontally oriented geometries

This section presents the ANOVA findings and regression equations based on the data of heat sinks arranged vertically using the Box-Behnken technique. Equations 6, 7, and 8 provide the RSM-derived equations for the results obtained from the aforementioned graphs. The Box-Behnken method is employed to analyze the design parameters and derive equations for a case involving seven different parameters: density, viscosity, specific heat, thermal conductivity, block thickness, block distances, and inlet pressure boundary conditions. The obtained equations are used to determine the average CPU temperature, thermal resistance, and Performance Evaluation Criteria (PEC). The R^2 value indicates the effectiveness of the obtained equations. The equations derived from the results of R_{th}, T_m, and PEC parameters in horizontal arrangements have R^2 values of 99.21%, 99.21%, and 99.37%, respectively. These results indicate that the equations and the numerical results obtained through the FLUENT program are reliable. The ANOVA statistical results are presented in Tables 2, 3, and 4 for R_{th}, T_m, and PEC. These tables demonstrate that the F statistical values of the model were significantly high for each response, and the p-value is generally less than 0.001, showing a strong match between each answer and the related model equations. Typically, p-values below 0.001 suggest that the model is statistically significant with a 99% confidence level. The tables clearly indicate that the linear, square, and cubic effects of each variable have a substantial impact on each answer. This is evident from the probability values of each effect, all of which are below 0.05.

$$R_{th} = 0.371 + 0.000011 \, \rho + 18.8 \, \mu - 0.367 \, a + 0.1052 \, s - 0.000049 \, P_{inlet} - 0.000014 \, \rho*a + \quad (6)$$
$$0.000031 \, \rho*s - 42.8 \, \mu*a + 65.3 \, \mu*s - 0.00937 \, \mu*P_{inlet} + 0.1009 \, a*s + 0.000021 \, a*P_{inlet} - 0.000029 \, s*P_{inlet}$$

$$T_m = 311.12 + 0.00032 \, \rho + 564 \, \mu - 11.02 \, a + 3.16 \, s - 0.001461 \, P_{inlet} - 0.00041 \, \rho*a + 0.00092 \, \rho*s - \quad (7)$$
$$1283 \, \mu*a + 1960 \, \mu*s - 0.281 \, \mu*P_{inlet} + 3.028 \, a*s + 0.000638 \, a*P_{inlet} - 0.000866 \, s*P_{inlet}$$

$$PEC = -0.05 \quad + 0.000832\rho \quad + 23.1\mu \quad + 0.693 \, a + 0.179 \, s - 0.000096 \, P_{inlet} \quad + 0.000348 \, \rho*a - \quad (8)$$
$$0.000263 \, \rho*s + 17\mu*a \quad - 37.5 \, \mu*s \quad - 0.00328 \, \mu*P_{inlet} \quad - 0.4790 \, a*s \quad -$$
$$0.000056 a*P_{inlet} + 0.000046 s*P_{inlet}$$

Table 2. ANOVA results of R_{th}

Source	DF	Adj. SS	Adj. MS	F-Value	P-Value
Model	15	0.408581	0.027239	466.20	0.000
Linear	5	0.344179	0.068836	1178.14	0.000
ρ	1	0.000036	0.000036	0.61	0.439
μ	1	0.003143	0.003143	53.79	0.000
a	1	0.089761	0.089761	1536.28	0.000
s	1	0.132372	0.132372	2265.58	0.000
Pinlet	1	0.118461	0.118461	2027.48	0.000
Square	1	0.016635	0.016635	284.72	0.000
Pinlet*Pinlet	1	0.016635	0.016635	284.72	0.000
2-Way Interaction	9	0.007855	0.000873	14.94	0.000
ρ*a	1	0.000001	0.000001	0.01	0.903
ρ*s	1	0.000012	0.000012	0.20	0.653
ρ*Pinlet	1	0.000042	0.000042	0.72	0.399
μ*a	1	0.000038	0.000038	0.64	0.425
μ*s	1	0.000244	0.000244	4.18	0.046
μ*Pinlet	1	0.000113	0.000113	1.93	0.170
a*s	1	0.001032	0.001032	17.66	0.000
a*Pinlet	1	0.001026	0.001026	17.56	0.000
s*Pinlet	1	0.005251	0.005251	89.87	0.000
Error	56	0.003272	0.000058		
Total	71	0.411853			

Table 3. ANOVA results of T_m

Source	DF	Adj. SS	Adj. MS	F-Value	P-Value
Model	15	367.723	24.515	466.20	0.000
Linear	5	309.762	61.952	1178.14	0.000
ρ	1	0.032	0.032	0.61	0.439
μ	1	2.828	2.828	53.79	0.000
a	1	80.785	80.785	1536.28	0.000
s	1	119.135	119.135	2265.58	0.000
Pinlet	1	106.615	106.615	2027.48	0.000
Square	1	14.972	14.972	284.72	0.000
Pinlet*Pinlet	1	14.972	14.972	284.72	0.000
2-Way Interaction	9	7.069	0.785	14.94	0.000
ρ*a	1	0.001	0.001	0.01	0.903
ρ*s	1	0.011	0.011	0.20	0.653
ρ*Pinlet	1	0.038	0.038	0.72	0.399
μ*a	1	0.034	0.034	0.64	0.425
μ*s	1	0.220	0.220	4.18	0.046
μ*Pinlet	1	0.101	0.101	1.93	0.170
a*s	1	0.929	0.929	17.66	0.000
a*Pinlet	1	0.923	0.923	17.56	0.000
s*Pinlet	1	4.726	4.726	89.87	0.000
Error	56	2.945	0.053		
Total	71	370.668			

Table 4. ANOVA results of PEC

Source	DF	Adj. SS	Adj. MS	F-Value	P-Value
Model	15	0.958494	0.063900	590.10	0.000
Linear	5	0.767034	0.153407	1416.69	0.000
ρ	1	0.047884	0.047884	442.21	0.000
μ	1	0.000530	0.000530	4.89	0.031
a	1	0.171594	0.171594	1584.64	0.000
s	1	0.237078	0.237078	2189.39	0.000
Pinlet	1	0.310144	0.310144	2864.14	0.000
Square	1	0.031428	0.031428	290.23	0.000
Pinlet*Pinlet	1	0.031428	0.031428	290.23	0.000
2-Way Interaction	9	0.047179	0.005242	48.41	0.000
ρ*a	1	0.000551	0.000551	5.09	0.028
ρ*s	1	0.000876	0.000876	8.09	0.006
ρ*Pinlet	1	0.001454	0.001454	13.42	0.001
μ*a	1	0.000006	0.000006	0.06	0.815
μ*s	1	0.000081	0.000081	0.74	0.392
μ*Pinlet	1	0.000014	0.000014	0.13	0.722
a*s	1	0.023227	0.023227	214.49	0.000
a*Pinlet	1	0.007195	0.007195	66.44	0.000
s*Pinlet	1	0.013341	0.013341	123.20	0.000
Error	56	0.006064	0.000108		
Total	71	0.964558			

5.2. Findings from vertically oriented geometries

This section presents the ANOVA findings and regression equations based on the data of heat sinks arranged horizontally using the Box-Behnken technique. Equations 9, 10, and 11 provide the equations generated from the RSM for the findings seen in the previous graphics. The equations resulting from the analysis of R_{th}, T_m, and PEC parameters in horizontal configurations exhibit R^2 values of, 97.66%,

97.66%, and 98.45%, respectively. The R^2 results demonstrate parallelism with the values obtained in the horizontal arrangement and exceed a high threshold of 99%, indicating a strong correlation between the results obtained from FLUENT. The ANOVA statistical results are presented in Tables 5, 6, and 7. The tables reveal that the F statistical values of the model were considerably high for each response, with p-values typically below 0.001, indicating a good correlation between each answer and the corresponding model equations. A p-value < 0.001 indicates statistical significance at a 99% confidence level. The tables clearly show that the linear, square, and cubic impacts of each variable significantly influence each solution. The probability values of many effects are less than 0.05, indicating a clear trend.

$$R_{th} = -1.310 + 0.001698\,\rho + 348\,\mu + 0.048\,a + 0.397\,s + 0.000256\,P_{inlet} + 0.000160\,\rho*a - 0.000234\,\rho*s \quad (9)$$
$$- 49\,\mu*a - 80.8\,\mu*s - 0.0480\,\mu*P_{inlet} - 0.1495\,a*s - 0.000015\,a*P_{inlet} + 0.000000\,s*P_{inlet}$$

$$T_m = 260.70 + 0.05093\,\rho + 10446\,\mu + 1.4\,a + 11.90\,s + 0.00768\,P_{inlet} + 0.000001\,P_{inlet}*P_{inlet} \quad (10)$$
$$+ 0.0048\rho*a - 0.00701\,\rho*s - 0.000012\,\rho*P_{inlet} - 1463\,\mu*a - 2425\,\mu*s - 1.441\,\mu*P_{inlet} -$$
$$4.49\,a*s - 0.000461\,a*P_{inlet} + 0.000013\,s*P_{inlet}$$

$$PEC = -0,154 + 0,000835\,\rho + 154,1\,\mu + 0,191\,a + 0,109\,s - 0,000017\,P_{inlet} + 0,000003\,\rho \quad (11)$$
$$*a - 0,000064\,\rho*s + 184,2\,\mu*a - 125,6\,\mu*s - 0,0272\,\mu*P_{inlet} - 0,0563\,a*s -$$
$$0,000053\,a*P_{inlet} + 0,000017\,s*P_{inlet}$$

Table 5. ANOVA results of R_{th}

Source	DF	Adj. SS	Adj. MS	F-Value	P-Value
Model	15	1.22112	0.081408	158.84	0.000
Linear	5	0.87168	0.174335	340.15	0.000
ρ	1	0.05420	0.054195	105.74	0.000
μ	1	0.01104	0.011037	21.53	0.000
a	1	0.00481	0.004812	9.39	0.003
s	1	0.00001	0.000006	0.01	0.912
Pinlet	1	0.79192	0.791920	1545.15	0.000
Square	1	0.07331	0.073314	143.05	0.000
Pinlet*Pinlet	1	0.07331	0.073314	143.05	0.000
2-Way Interaction	9	0.06422	0.007136	13.92	0.000
ρ*a	1	0.00012	0.000117	0.23	0.635
ρ*s	1	0.00069	0.000693	1.35	0.250
ρ*Pinlet	1	0.04496	0.044963	87.73	0.000
μ*a	1	0.00005	0.000050	0.10	0.757
μ*s	1	0.00038	0.000379	0.74	0.393
μ*Pinlet	1	0.00305	0.003052	5.96	0.018
a*s	1	0.00229	0.002288	4.46	0.039
a*Pinlet	1	0.00055	0.000549	1.07	0.305
s*Pinlet	1	0.00000	0.000001	0.00	0.961
Error	57	0.02921	0.000513		
Lack-of-Fit	56	0.02231	0.000398	0.06	1.000
Pure Error	1	0.00690	0.006904		
Total	72	1.25033			

Table 6. ANOVA results of T_m

Source	DF	Adj. SS	Adj. MS	F-Value	P-Value
Model	15	1099.01	73.267	158.84	0.000
Linear	5	784.51	156.902	340.15	0.000
ρ	1	48.78	48.776	105.74	0.000
μ	1	9.93	9.933	21.53	0.000
a	1	4.33	4.331	9.39	0.003
s	1	0.01	0.006	0.01	0.912
Pinlet	1	712.73	712.728	1545.15	0.000
Square	1	65.98	65.982	143.05	0.000
Pinlet*Pinlet	1	65.98	65.982	143.05	0.000
2-Way Interaction	9	57.80	6.422	13.92	0.000
ρ*a	1	0.11	0.105	0.23	0.635
ρ*s	1	0.62	0.624	1.35	0.250
ρ*Pinlet	1	40.47	40.466	87.73	0.000
μ*a	1	0.04	0.045	0.10	0.757
μ*s	1	0.34	0.341	0.74	0.393
μ*Pinlet	1	2.75	2.747	5.96	0.018
a*s	1	2.06	2.059	4.46	0.039
a*Pinlet	1	0.49	0.494	1.07	0.305
s*Pinlet	1	0.00	0.001	0.00	0.961
Error	57	26.29	0.461		
Lack-of-Fit	56	20.08	0.359	0.06	1.000
Pure Error	1	6.21	6.213		
Total	72	1125.30			

Table 7. ANOVA results of PEC

Source	DF	Adj. SS	Adj. MS	F-Value	P-Value
Model	15	0.587599	0.039173	241.49	0.000
Linear	5	0.472862	0.094572	583.01	0.000
rho	1	0.054982	0.054982	338.95	0.000
mu	1	0.000185	0.000185	1.14	0.290
a	1	0.050785	0.050785	313.07	0.000
s	1	0.022769	0.022769	140.36	0.000
Pinlet	1	0.344361	0.344361	2122.89	0.000
Square	1	0.036230	0.036230	223.35	0.000
Pinlet*Pinlet	1	0.036230	0.036230	223.35	0.000
2-Way Interaction	9	0.015621	0.001736	10.70	0.000
rho*a	1	0.000000	0.000000	0.00	0.987
rho*s	1	0.000053	0.000053	0.32	0.571
rho*Pinlet	1	0.002693	0.002693	16.60	0.000
mu*a	1	0.000709	0.000709	4.37	0.041
mu*s	1	0.000915	0.000915	5.64	0.021
mu*Pinlet	1	0.000981	0.000981	6.05	0.017
a*s	1	0.000325	0.000325	2.00	0.163
a*Pinlet	1	0.006573	0.006573	40.52	0.000
s*Pinlet	1	0.001788	0.001788	11.02	0.002
Error	57	0.009246	0.000162		
Lack-of-Fit	56	0.008367	0.000149	0.17	0.981
Pure Error	1	0.000879	0.000879		
Total	72	0.596845			

While the increase in the gap between the blocks seen in the horizontal arrangement has a positive effect on PEC, it is also seen in the vertical arrangement that it has a negative effect on R_{th} and T_m, that is, it increases.

6. Conclusion

In this study, the RSM method was applied to the data obtained with the effect of using three different fluid types (water, CuO, and CuO+Fe/Water) in heat sinks designed in different thicknesses and cavity block types. The findings obtained are as follows:

1. The R^2 values obtained in the horizontal arrangement are 99.21%, 99.21%, and 99.37% for R_{th}, T_m, and PEC, and 97.66%, 97.66%, and 98.45%, in the vertical arrangement. It is a remarkable result that all data are higher than 99%.

2. It was observed that increasing the distance between the blocks increased the PEC, i.e., had a positive effect but had a negative effect on R_{th} and T_m.

3. It is seen that increasing the block thickness has a very serious effect on R_{th} and T_m; that is, it increases the cooling capacity and uniformizes the temperature distribution.

7. Author Contribution Statement

Taha Tuna Göksu: Conceptualization, Data curation, Formal analysis, Investigation, Methodology, Validation, Visualization, Writing – original draft, Writing - review & editing.

8. Ethics Committee Approval and Conflict of Interest

"There is no conflict of interest with any person/institution in the prepared article"

9. Nomenclature

C_p	specific heat, (J/kg·K)
D_h	hydraulic diameter, (m)
f	friction factor
h	convection heat transfer coefficient, (W/m²·K)
k	thermal conductivity, (W/m.K)
q''	heat flux, (W/m²)
R_{th}	effective thermal resistance (K/W)
T	temperature, (K)
Greeks	
μ	dynamic viscosity, (Pa·s)
ρ	density, (kg/m³)
φ	concentration (%)
Abbreviations	
CFD	computational fluid dynamics
CPU	central processing unit
PEC	performance evaluation criterion
RSM	response surface method

10. References

[1] J. Ajayan, D. Nirmal, S. Tayal, S. Bhattacharya, L. Arivazhagan, A.S. Ausgustine, P. Murugapandiyann and D. Ajitha, "Nanosheet field effect transistors-A next generation device to keep Moore's law alive: An intensive study", Microel. Jour., vol. 114, p. 105141, Aug. 2021.

[2] A. Matallana, E. Ibarra, I. Lopez, J. Andreu, J. I. Garate, X. Jorda and J. Rebollo, "Power module electronics in HEV/EV applications: New trends in wide-bandgap semiconductor technologies and design aspects," Renew. and Sust. Ener. Reviews, vol. 113, p. 109264, Oct. 2019.

[3] R. R. L, P. Jayaramu, S. Gedupudi, and S. K. Das, "Experimental investigation of the influence of boiling-induced ageing on high heat flux flow boiling in a copper microchannel," International Journal of Heat and Mass Transfer, vol. 181, p. 121862, Dec. 2021.

[4] Gholami,A. and Bahrami, M., "Thermal spreading resistance inside anisotropic plates with arbitrarily located hotspots".

[5] K.-S. Yang, C.-H. Chung, C.-W. Tu, C.-C. Wong, T.-Y. Yang, and M.-T. Lee, "Thermal spreading resistance characteristics of a high power light emitting diode module," Appl. Ther.Eng., vol. 70, no. 1, pp. 361–368, Sep. 2014.

[6] A. F. Al-Neama, N. Kapur, J. Summers, and H. M. Thompson, "Thermal management of GaN HEMT devices using serpentine minichannel heat sinks," Appl. Ther. Eng., vol. 140, pp. 622–636, Jul. 2018.

[7] H.-C. Chiu, R.-H. Hsieh, K. Wang, J.-H. Jang, and C.-R. Yu, "The heat transfer characteristics of liquid cooling heat sink with micro pin fins," Inter. Commun.in Heat and Mass Transfer, vol. 86, pp. 174–180, Aug. 2017.

[8] H.-C. Chiu, M.-J. Youh, R.-H. Hsieh, J.-H. Jang, and B. Kumar, "Numerical investigation on the temperature uniformity of micro-pin-fin heat sinks with variable density arrangement," Case Stud.in Ther. Engi., vol. 44, p. 102853, Apr. 2023.

[9] A. Shahsavar, M. Shahmohammadi, and I. Baniasad Askari, "The effect of inlet/outlet number and arrangement on hydrothermal behavior and entropy generation of the laminar water flow in a pin-fin heat sink," Inter. Commun. in Heat and Mass Transfer, vol. 127, p. 105500, Oct. 2021.

[10] A. Shahsavar, M. Shahmohammadi, and I. B. Askari, "CFD simulation of the impact of tip clearance on the hydrothermal performance and entropy generation of a water-cooled pin-fin heat sink," Intern. Commun. in Heat and Mass Transfer, vol. 126, p. 105400, Jul. 2021.

[11] R. Fattahi and M. Saidi, "Numerical investigation of curved shape fins height effect on heat transfer and flow characteristics in open microchannel heat sink," Inter.Jour. of Thermal Sci., vol. 185, p. 108060, Mar. 2023.

[12] Y. Xia, L. Chen, J. Luo, and W. Tao, "Numerical investigation of microchannel heat sinks with different inlets and outlets based on topology optimization," Appl. Ener., vol. 330, p. 120335, Jan. 2023.

[13] O. A. Ismail, A. M. Ali, M. A. Hassan, and O. Gamea, "Geometric optimization of pin fins for enhanced cooling in a microchannel heat sink," Intern. Jour.of Ther., Sci., vol. 190, p. 108321, Aug. 2023.

[14] F. Koca and T. B. Güder, "Numerical investigation of CPU cooling with micro-pin–fin heat sink in different shapes," Eur. Phys. J. Plus, vol. 137, no. 11, p. 1276, Nov. 2022.

[15] R. B. Gurav, P. Purohit, P. K. Tamkhade, and S. P. Nalavade, "Computational and analytical study on CPU heat sink cooling by single and double stack air-foil micro pin fins," Mater. Today: Procee., p. S2214785323011719, Mar. 2023.

[16] F. N. Ghadhban and H. M. Jaffal, "Numerical and experimental thermohydraulic performance evaluation of multi-minichannel heat sinks considering channel structure modification," Inter. Commun.s in Heat and Mass Transfer, vol. 145, p. 106847, Jun. 2023.

[17] A. J. Obaid and V. M. Hameed, "An experimental and numerical comparison study on a heat sink thermal performance with new fin configuration under mixed convective conditions," South African Jour. of Chem. Eng., vol. 44, pp. 81–88, Apr. 2023.

[18] M. Fathi, M. M. Heyhat, M. Zabetian Targhi, and S. Bigham, "Bifurcated divergent microchannel heat sinks for enhanced micro-electronic cooling," Inter. Commun. in Heat and Mass Transfer, vol. 146, p. 106868, Jul. 2023.

[19] G. Sung, D.-Y. Na, and S.-J. Yook, "Enhancement of the cooling performance of a pin fin heat sink based on the chimney effect using aluminum tape," Inter. Jour. of Heat and Mass Transfer, vol. 201, p. 123613, Feb. 2023.

[20] M. W. Uddin and N. S. Sifat, "Comparative study on hydraulic and thermal characteristics of minichannel heat sink with different secondary channels in parallel and counter flow directions," Inter. Jour.of Thermof., vol. 17, p. 100296, Feb. 2023.

[21] V. Arumuru, K. Rajput, R. Nandan, P. Rath, and M. Das, "A novel synthetic jet based heat sink with PCM filled cylindrical fins for efficient electronic cooling," Jour. of Ener. Stor., vol. 58, p. 106376, Feb. 2023.

[22] T. T. Göksu and F. Yılmaz, "Numerical comparison study on heat transfer enhancement of different cross-section wire coils insert with varying pitches in a duct," Jour. of Ther. Eng., vol. 7, no. 7, Art. no. 7, Nov. 2021.

[23] İ. H. Yılmaz and T. T. Göksu, "Enhancement of heat transfer using twisted tape insert in a plain tube," Bitlis Eren Üni. Fen Bilim. Derg., vol. 8, no. 1, Art. no. 1, Mar. 2019.

[24] Kavitha. C, M. P.C., and A. K. C.M, "Numerical study on the performance of Al2O3/water nanofluids as a coolant in the fin channel heat sink for an electronic device cooling," Mater. Today: Procee., p. S221478532300901X, Mar. 2023.

[25] Choi, S. U. S., Singer, D. A., and Wang, H. P., "Developments and applications of non-Newtonian flows," vol. 66, no. 99–105, 1995.

[26] Chol, S., "Enhancing thermal conductivity of fluids with nanoparticles," ASME, vol. 231, 1995.

[27] Xinyu, W., Huiying, W., and Ping, C., "Pressure drop and heat transfer of Al2O3-H2O nanofluids through silicon microchannel," Jour.of Micromec. and Microeng., vol. 19, p. 105020.

[28] S. S. Ghadikolaei, S. Siahchehrehghadikolaei, M. Gholinia, and M. Rahimi, "A CFD modeling of heat transfer between CGNPs/H2O Eco-friendly nanofluid and the novel nature-based designs heat sink: Hybrid passive techniques for CPU cooling," Ther. Sci. and Eng.Progress, vol. 37, p. 101604, Jan. 2023.

[29] M. Khoshvaght-Aliabadi, P. Ghodrati, H. Mortazavi, and Y. T. Kang, "Numerical analysis of heat transfer and flow characteristics of supercritical CO2-cooled wavy mini-channel heat sinks," App. Ther. Eng., vol. 226, p. 120307, May 2023.

[30] M. D. Massoudi and M. B. Ben Hamida, "Combined impacts of square fins fitted wavy wings and micropolar magnetized-radiative nanofluid on the heat sink performance," Journal of Mag. and Mag. Mater., vol. 574, p. 170655, May 2023.

[31] H. R. Seyf and M. Feizbakhshi, "Computational analysis of nanofluid effects on convective heat transfer enhancement of micro-pin-fin heat sinks," Inter.Jour.of Ther. Sci., vol. 58, pp. 168–179, Aug. 2012.

[32] T. Ambreen, A. Saleem, and C. W. Park, "Pin-fin shape-dependent heat transfer and fluid flow characteristics of water- and nanofluid-cooled micropin-fin heat sinks: Square, circular and triangular fin cross-sections," App. Ther.Eng., vol. 158, p. 113781, Jul. 2019.

[33] W. Cai et al., "Eulerian-Lagrangian investigation of nanoparticle migration in the heat sink by considering different block shape effects," App. Ther. Eng., vol. 199, p. 117593, Nov. 2021.

[34] M. Yasir, M. Khan, A. S. Alqahtani, and M. Y. Malik, "Numerical study of axisymmetric hybrid nanofluid MgO-Ag/H2O flow with non-uniform heat source/sink," Alex. Eng. Jour., vol. 75, pp. 439–446, Jul. 2023.

[35] S. Mukherjee, S. Wciślik, V. Khadanga, and P. C. Mishra, "Influence of nanofluids on the thermal performance and entropy generation of varied geometry microchannel heat sink," Case Stud. in Ther. Eng., vol. 49, p. 103241, Sep. 2023.

[36] O. Ozbalci, A. Dogan, and M. Asilturk, "Performance of discretely mounted metal foam heat sinks in a channel with nanofluid," App. Ther. Eng., vol. 235, p. 121375, Nov. 2023.

[37] I. Karaaslan and T. Menlik, "Numerical study of a photovoltaic thermal (PV/T) system using mono and hybrid nanofluid," Solar Ener., vol. 224, pp. 1260–1270, Aug. 2021.

[38] C. J. Ho, J.-K. Peng, T.-F. Yang, S. Rashidi, and W.-M. Yan, "On the assessment of the thermal performance of microchannel heat sink with nanofluid," Inter. Jour. of Heat and Mass Transfer, vol. 201, p. 123572, Feb. 2023.

[39] G. Sriharan, S. Harikrishnan, and H. F. Oztop, "Performance improvement of the mini hexagonal tube heat sink using nanofluids," Ther. Sci. and Eng. Prog., vol. 34, p. 101390, Sep. 2022.

[40] S. E. Ghasemi, A. A. Ranjbar, and M. J. Hosseini, "Forced convective heat transfer of nanofluid as a coolant flowing through a heat sink: Experimental and numerical study," Jour. of Mol. Liq., vol. 248, pp. 264–270, Dec. 2017.

[41] S. E. Ghasemi, A. A. Ranjbar, and M. J. Hosseini, "Thermal and hydrodynamic characteristics of water-based suspensions of Al2O3 nanoparticles in a novel minichannel heat sink," Jour. of Mol. Liq., vol. 230, pp. 550–556, Mar. 2017.

[42] M. Bahiraei, S. Heshmatian, and M. Keshavarzi, "Multi-criterion optimization of thermohydraulic performance of a mini pin fin heat sink operated with ecofriendly graphene nanoplatelets nanofluid considering geometrical characteristics," Jour. of Mol. Liq., vol. 276, pp. 653–666, Feb. 2019.

[43] W. Guo, G. Li, Y. Zheng, and C. Dong, "Numerical study of nanofluids thermal and hydraulic characteristics considering Brownian motion effect in micro fin heat sink," Jour. of Mol. Liq., vol. 264, pp. 38–47, Aug. 2018.

[44] M. Bahiraei, M. Jamshidmofid, and M. Goodarzi, "Efficacy of a hybrid nanofluid in a new microchannel heat sink equipped with both secondary channels and ribs," Jour. of Mol. Liq., vol. 273, pp. 88–98, Jan. 2019.

[45] N. Abbas, W. Shatanawi, and K. Abodayeh, "Computational Analysis of MHD Nonlinear Radiation Casson Hybrid Nanofluid Flow at Vertical Stretching Sheet," Symmetry, vol. 14, no. 7, Art. no. 7, Jul. 2022.

[46] B. Cabir and A. Yakın, "Evaluation of gasoline-phthalocyanines fuel blends in terms of engine performance and emissions in gasoline engines," Jour. of the Ener. Inst., vol. 112, p. 101483, Feb. 2024.

[47] M. Yetkin, Ö. F. Taş, and E. Sayın, "Comparison of equivalent earthquake load method for TEC-2007 and TBEC-2018: Adıyaman province example," Firat Univ. Jour.of Exper. and Comp. Eng, vol. 2, no. 2, Art. no. 2, Jun. 2023.

[48] T. T. Göksu, "Investigation of pin and perforated heatsink cooling efficiency and temperature distribution," J Therm Anal Calorim, Apr. 2024.

[49] J. Zhou, M. Hatami, D. Song, and D. Jing, "Design of microchannel heat sink with wavy channel and its time-efficient optimization with combined RSM and FVM methods," Inter. Jour. of Heat and Mass Transfer, vol. 103, pp. 715–724, Dec. 2016.

[50] M. Rahimi-Gorji, O. Pourmehran, M. Hatami, and D. D. Ganji, "Statistical optimization of microchannel heat sink (MCHS) geometry cooled by different nanofluids using RSM analysis," Eur. Phys. J. Plus, vol. 130, no. 2, p. 22, Feb. 2015.

[51] M. Shanmugam and L. Sirisha Maganti, "Multi-objective optimization of parallel microchannel heat sink with inlet/outlet U, I, Z type manifold configuration by RSM and NSGA-II," Inter. Jour.of Heat and Mass Transfer, vol. 201, p. 123641, Feb. 2023.

[52] F. Pourfattah, M. F. Kheryrabadi, and L.-P. Wang, "Coupling CFD and RSM to optimize the flow and heat transfer performance of a manifold microchannel heat sink," J Braz. Soc. Mech. Sci. Eng., vol. 45, no. 3, p. 178, Mar. 2023.

[53] T. T. Göksu, "Enhancing cooling efficiency: Innovative geometric designs and mono-hybrid nanofluid applications in heat sinks," Case Stud. in Ther. Eng., vol. 55, p. 104096, Mar. 2024.

[54] S. Lineykin and S. Ben-Yaakov, "Mod. and Anal. of Therm. Modules," IEEE Transactions on Industry Applications, vol. 43, no. 2, pp. 505–512, Mar. 2007.

[55] R. L. Webb, "Performance evaluation criteria for use of enhanced heat transfer surfaces in heat exchanger design," International Journal of Heat and Mass Transfer, vol. 24, no. 4, pp. 715–726, Apr. 1981.

[56] K. Martin, A. Sözen, E. Çiftçi, and H. M. Ali, "An Experimental Investigation on Aqueous Fe–CuO Hybrid Nanofluid Usage in a Plain Heat Pipe," Int J Thermophys, vol. 41, no. 9, p. 135, Sep. 2020.